ELSEVIER

International Journal of Mass Spectrometry 223–224 (2003) 169–177

International Journal of Mass Spectrometry

www.elsevier.com/locate/ijms

State selectivity in collisional electron-transfer processes involving the NO molecule

Detlef Schröder*, Helmut Schwarz

Institut für Chemie, Technische Universität Berlin, D-10623 Berlin, Germany

Received 17 January 2002; accepted 22 March 2002

In memory of Werner Lindinger.

Abstract

Collisional electron transfer at kiloelectron-volt energies involving the NO molecule in various charge states is probed by tandem mass spectrometry. Unlike many other molecules, singly charged $NO^{-/+}$ ions can be subjected to all conceivable kinds of neutralization–reionization (NR) and charge reversal (CR) sequences. Because all these experiments involve electron transfer to or from the NO unit, we may generally term them as electron-transfer mass spectrometry (ET-MS). Moreover, the fact that $NO^{-/+}$ ions give rise to distinct survivor ion signals in all NR and CR spectra permits a detailed analysis of the ET processes occurring by means of energy-resolved experiments. Inter alia, these measurements reveal that the seemingly identical transitions of the anionic species to the cation, i.e., $NO^- \rightarrow NO^\bullet \rightarrow NO^+$ occurring in NR and $NO^- \rightarrow NO^+$ occurring in CR, are associated with rather pronounced differences as far as the populations of electronic states of the resulting NO^+ cations are concerned. (Int J Mass Spectrom 223–224 (2003) 169–177)
© 2002 Elsevier Science B.V. All rights reserved.

Keywords: Charge reversal; Electron transfer; Mass spectrometry; Neutralization–reionization; Nitrogen monoxide

1. Introduction

As a prototype diatomic molecule, the chemistry and physics of excited states of NO^+ have been of wide interest for quite a long time [1]. Particular attention has been paid to relaxation processes [2–4], and Werner Lindinger was one of the pioneers in this area [5,6]. As nitrogen monoxide is a stable neutral radical, it has been examined at great length, and the details of the potential energy surfaces of $NO^{-/0/+}$ are well established. Here, we use an adiabatic electron affinity of $EA_a = 0.026\,eV$ [7] and an adiabatic ionization energy of $IE_a = 9.264\,eV$ [8]. Not surprisingly, nitrogen monoxide was also studied extensively by mass spectrometric means, and already the very early charge-stripping (CS) experiments of Cooks et al. revealed composite peaks due to the presence of excited states of NO^+ [9].

In 1998, we introduced the neutral-and-ion decomposition difference (NIDD) scheme [10–13] as a method to examine the reactivity of transient neutrals by mass spectrometric means. The essence of the NIDD scheme is the qualitative analysis of neutralization–reionization (NR) [14] and charge-reversal (CR) [15,16] spectra obtained under comparable conditions. In one of our initial studies, nitrogen monoxide ions were chosen to test the performance of the NIDD

* Corresponding author.
E-mail: detlef.schroeder@www.chem.tu-berlin.de

1387-3806/02/$ – see front matter © 2002 Elsevier Science B.V. All rights reserved.
PII S1387-3806(02)00788-1

approach for selected diatomic molecules [13]. Based on the negligible NIDD intensities for NO^+ and NO^- ions, we concluded that, irrespective of the actual charge state, there exist no pronounced differences between the NR and CR processes occurring for this particular molecule. As our contribution to an issue in the memory of the scientific oeuvre of the late Werner Lindinger, we report some energy-resolved experiments which reveal that the NIDD behavior of the NO molecule is not as simple as we have anticipated before.

2. Experimental details

The experiments employed a VG-ZAB-2HF/AMD 604 four-sector mass spectrometer of *BEBE* configuration (*B* stands for magnetic and *E* for electric sector) which has been described elsewhere [17]. NO^- anions were prepared by dissociative chemical ionization (CI, electron energy 100 eV, repeller voltage ca. 0 V) of N_2O. NO^+ cations were generated by electron ionization (EI, electron energy 70 eV, repeller voltage ca. 20 V) of either NO or N_2O. Further, nitrogen monoxide was ionized with electrons having only 15 eV kinetic energy (with the repeller grounded to the source potential [18]), thereby avoiding the formation of electronically excited cation states (see below). The ions of interest, having ca. 8 keV kinetic energy, were mass-selected using either *B*(1) only or *B*(1)/*E*(1) at mass resolutions of $m/\Delta m = 2000$–6000, sufficient to resolve isobaric impurities.

The energy-resolved NR and CR experiments discussed below were performed in the tandem collision cells located in the field-region between *B*(1) and *E*(1). To this end, *B*(1) mass-selected precursor ions were collided with the target gases specified below at ca. 80% transmission of the incident ion beam, and the sector *E*(1) was adjusted to the desired charge. In the NR experiments, a deflector electrode located between the two collision cells was floated to 1 kV. In $^-NR^-$, the target gases were a combination of oxygen for neutralization and xenon for reionization. Oxygen was used in both collisions in $^-NR^+$, and $^-CR^+$ was performed using oxygen in either only one or both collision cells. Likewise, only xenon was used as collision gas in $^+NR^-$ and $^+CR^-$, respectively. Finally, $^+NR^+$ applied the frequently used combination of xenon for neutralization and oxygen for reionization. Briefly spoken, xenon is used to add and oxygen to remove an electron from the projectile in these CR and NR experiments. In addition to xenon and oxygen, several other rare gases as well as nitrogen monoxide were used as target gases, but no major differences were observed. The corresponding NIDD spectra were derived from the difference of the NR and CR spectra as described in [10–13]; briefly, the normalized intensities (I_i) of the CR spectra are subtracted from those in the corresponding NR spectra, i.e., $I_i(\mathrm{NIDD}) = [I_i(\mathrm{NR})/\Sigma_i I_i(\mathrm{NR})] - [I_i(\mathrm{CR})/\Sigma_i I_i(\mathrm{CR})]$.

The energy balances of the kiloelecton-volt-collision experiments were determined from the high-energy onsets of the parent ion and the NR and CR survivor signals, respectively, where the term "survivor" stands for those species which successfully undergo the redox transitions under study. The kinetic energy scale of the sector *E*(1) was calibrated using the following transitions as references (i) $X^- \rightarrow X^+$ for X = F–I and $O_2^- \rightarrow O_2^+$ in $^-NR^+$ as well as $^-CR^+$, (ii) $X^+ \rightarrow X^-$ for X = Cl–I and $O_2^+ \rightarrow O_2^-$ in $^+NR^-$ as well as $^+CR^-$, (iii) $X^- \rightarrow X^-$ in $^-NR^-$, and (iv) $N_2^+ \rightarrow N_2^+$ as well as $O_2^+ \rightarrow O_2^+$ in $^+NR^+$, respectively. In the related energy-resolved CS technique [19] there is an ongoing debate, whether multiplicative or additive correction schemes are more appropriate [20]; our recent results indicate that the multiplicative approach is more appropriate in our instrument [21]. For experiments in which the charge is reversed, application of an additive correction is certainly required, because a given component of the ion optics will precisely work in the opposite direction for cations and anions, respectively. Note that a decisive choice between these two calibrations schemes cannot be made for the time being. As a compromise, the actual calibration schemes therefore used two parameters $\Delta E = c + f\,\Delta E_{\mathrm{exp}}$, where c and f were determined by calibration with the reference transitions mentioned above.

3. Results and discussion

As mentioned previously [13], the overview NR and CR spectra of $NO^{-/+}$ are almost identical, resulting in vanishing NIDD patterns (Table 1). Accordingly, one is tempted to conclude that the same species are formed, i.e., the same electronic state of the cation in this particular case. However, in addition to the dissociation behavior, NR and CR spectra can provide further information, if energy-resolved experiments are performed. In several previous studies, we have employed energy-resolved NR and CR measurements to unravel so far unknown redox properties of gaseous species [22–25] and/or to probe the nature of species formed in NR sequences [26–28]. Instead, here, we shall use the well-known $NO^{-/0/+}$ system to discuss the prospects and the limitations of these particular experiments which we wish to generally term as electron-transfer mass spectrometry (ET-MS).

3.1. Background

Before addressing the experimental data, it is indicated to recall some general aspects of the ET-MS experiments under study. Electron transfer in high-energy collisions is a highly non-adiabatic process which is best described to occur as a vertical transition. For example, 8 keV kinetic energy of an $NO^{+/-}$ ion correspond to a velocity of about 2×10^5 m/s such that passage of a target gas, having a typical cross-section in the order of ca. 5 Å^2, takes about 2×10^{-15} s. Electron-transfer processes occurring in these collisions are therefore governed by the associated Franck–Condon factors. In most cases, the observed redox processes are highly endothermic and driven by the kinetic energy of the projectile ion. This conversion of kinetic into potential energy leads to a shift of the resulting ion signals on the kinetic energy scale. Depending on the type of experiment performed, this is denoted as ΔE(NR) or ΔE(CR), respectively, where we use $\Delta E = E_{\text{parent}} - E_{\text{survivor}}$ such that ΔE is positive for endothermic electron transfer. Of course, a pivotal prerequisite is that a survivor ion is formed at all, which is by no means fulfilled for all species, but is the case for NO (see below). Primarily depending on parent and survivor ion intensities, the resolution of the ΔE measurements amounts to 0.5–4 eV, such that vibrational progressions cannot be resolved and also Franck–Condon envelopes can only be inferred from peak broadenings. Moreover, the absolute uncertainty of ΔE is ±0.2 eV at best [20] in conventional mass spectrometers; for ET-MS experiments with higher resolution, see [29]. In these respects, many spectroscopic techniques are clearly superior to energy-resolved ET-MS. Note, however, that the latter can be applied to any kind of mass-selected ions which gives rise to a significant survivor signal.

Let us now consider the energy balances of the various experiments [16] for a hypothetical species $A^{+/-}$ colliding with a quasi-stationary target gas T; note that only singly-charged projectile ions are considered here.

$$A^- + T \rightarrow A + T + e^- \quad \Delta E(^-N) = DE_v(A^-) \qquad (1)$$

$$A + T \rightarrow A^- + T^+ \quad \Delta E(R^-) = IE_v(T) - EA_v(A) \qquad (2)$$

Table 1
Fragment ions[a,b] observed in the NR and CR mass spectra[c] of NO^- anions generated by chemical ionization of N_2O and NO^+ cations generated by electron ionization of neutral NO and the resulting NIDD spectra[c,d]

	$NO^{+/-}$	$O^{+/-}$	$N^{+/-}$
$^-NR^-$	100	0.6	<0.2
$^-NR^+$	100	4.1	3.7
$^-CR^+$	100	3.4	3.2
$^-NIDD^+$[d]	−1.1	0.6	0.5
$^+NR^-$	100	0.9	<0.2
$^+CR^-$	100	1.1	<0.2
$^+NIDD^-$[d]	−0.2	0.2	
$^+NR^+$	100	0.7	0.6

[a] The charge states of the products NO, O, and N depend on the type of experiment performed.

[b] Given relative to the base peak (1 0 0). Figures behind the comma are within experimental error, but are given for the sake of consistency in the context of the NIDD data.

[c] The charges of the projectile and product ions are indicated as superscripts.

[d] NIDD intensities given as percentages; values below ±2% are considered to be insignificant; see [13].

Adding Eqs. (1) and (2), we get Eq. (3)

$$A^- + 2T \rightarrow A^- + T + T^+ + e^-$$
$$\Delta E(^-NR^-) = IE_v(T) + DE_v(A^-) - EA_v(A) \quad (3)$$

The energy balance of an $^-NR^-$ sequence ($A^- \rightarrow A \rightarrow A^-$) is given by Eqs. (1)–(3), where $DE_v(A^-)$ stands for the vertical electron detachment energy of the anion, $IE_v(T)$ for the vertical ionization energy of the target, and $EA_v(A)$ for the vertical electron affinity of neutral A. Note that none of these and numerous other experiments conducted so far in our laboratory provide evidence for electron transfer to the target gas, i.e., the formation of the T^-, and the possible contribution of $EA_v(T)$ is therefore not considered in the energy balances of the NR and CR experiments. In ET-MS experiments, only the overall energy balances are measured as the transient neutrals can only be detected via reionization. In order to further appreciate Eq. (3), let us consider two extreme cases. If $DE_v(A^-)$ and $EA_v(A)$ are similar, the difference between the associated vertical and adiabatic transitions is small, and we arrive at ($\Delta E(^-NR^-) \approx IE_v(T)$) or simply IE($T$) if an atomic target is used. Hence, energy-resolved $^-NR^-$ experiments are almost useless, because the target gas employed needs to be a stable neutral and much better methods exist for the determination of IE(T) in such a case. On the other hand, a $^-NR^-$ sequence is rather unlikely to yield a survivor signal for $DE_v(A^-) \gg EA_v(A)$ because this would result in unfavorable Franck–Condon factors. This is particularly true for reionization to anions because the latter are only formed efficiently when the corresponding neutral species exhibit significant vertical EAs. In fact, charge reversal of cations to anions ($^+CR^-$) can be used as a method to distinguish structural isomers of cationic species which are difficult to differentiate otherwise [30,31].

By and large similar arguments hold true for a $^+NR^+$ sequence ($A^+ \rightarrow A \rightarrow A^+$), Eqs. (4)–(6), where $RE_v(A^+)$ stands for the vertical recombination energy of the cation. If $RE_v(A^+)$ and $IE_v(A)$ are similar, Eq. (6) reduces to $\Delta E(^+NR^+) \approx IE_v(T)$ which is again trivial. Some information, but often of limited use, can be gained if $RE_v(A^+) \ll IE_v(A)$ because the observed effects can be related to the differences between vertical and adiabatic redox processes [27,32].

$$A^+ + T \rightarrow A + T^+$$
$$\Delta E(^+N) = IE_v(T) - RE_v(A^+) \quad (4)$$

$$A + T \rightarrow A + T + e^- \quad \Delta E(R^+) = IE_v(A) \quad (5)$$

Adding Eqs. (4) and (5), we get Eq. (6)

$$A^+ + 2T \rightarrow A^+ + T + T^+ + e^-$$
$$\Delta E(^+NR^+) = IE_v(T) + IE_v(A) - RE_v(A^+) \quad (6)$$

In marked contrast, valuable data about the redox behavior of $A^{-/0/+}$ can be gained when the net charges change in the course of the electron-transfer sequences. To a first approximation, the energy balance of a $^-NR^+$ sequence ($A^- \rightarrow A \rightarrow A^+$) is given by the combination of Eqs. (1) and (5) leading to Eq. (7) for the overall process.

$$A^- + 2T \rightarrow A^+ + 2T + 2e^-$$
$$\Delta E(^-NR^+) = DE_v(A^-) + IE_v(A) \quad (7)$$

While collisional electron detachment from anionic species in the first step is usually quite efficient at kiloelectron-volt energies, the resulting cationic survivor signals are often weak or even absent in ET-MS of anionic species [33]. The reason is that the binding characteristics and ion structures of anions and cations differ largely in many cases, leading to unfavorable Franck–Condon factors and often also low-lying dissociation channels at some charge state. Accordingly, often the difference between the vertical and adiabatic properties is significant, in that $\Delta E(^-NR^+) > EA_a(A) + IE_a(A)$.

Next, let us consider a $^-CR^+$ sequence ($A^- \rightarrow A^+$) in which a direct transition from the anion to the cation occurs without intermediate, resulting in Eq. (8), where $IE_v(A')$ is the vertical ionization energy of A at the geometry of the anion.

$$A^- + T \rightarrow A^+ + T + 2e^-$$
$$\Delta E(^-CR^+) = DE_v(A^-) + IE_v(A') \quad (8)$$

For experimental reasons, however, the contribution of the corresponding $^{-}NR^{+}$ sequence ($A^{-} \rightarrow A \rightarrow A^{+}$) cannot be avoided completely. In a strict sense, CR experiments always need to be considered as a superposition of CR and NR events, where the former predominate in most cases, however. As far as energy-resolved experiments are concerned, the onset of the $^{-}CR^{+}$ survivor may therefore be obscured by species formed via a $^{-}NR^{+}$ sequence [27].

Much more severe constraints are operative in $^{+}NR^{-}$ and $^{+}CR^{-}$ experiments, because they require the formation of anions which bear sufficient lifetime in order to be detected (several 10 μs). The corresponding energy balance of a $^{+}NR^{-}$ sequence ($A^{+} \rightarrow A \rightarrow A^{-}$) is given by adding Eqs. (2) and (4) to give Eq. (9).

$$A^{+} + 2T \rightarrow A^{-} + 2T^{+}$$
$$\Delta E(^{+}NR^{-}) = 2IE_{v}(T) - RE_{v}(A^{+}) - EA_{v}(A) \quad (9)$$

With T = xenon, this leads to $\Delta E(^{+}NR^{-}) = 24.26\,eV - (RE_{v}(A^{+}) + EA_{v}(A))$ and hence one is dealing with highly endothermic processes.

Even more energy is required in the corresponding $^{+}CR^{-}$ sequence ($A^{+} \rightarrow A^{-}$) in which the transition from the cation to the anion requires double ionization of the target T, Eq. (10).

$$A^{+} + T \rightarrow A^{-} + T^{2+}$$
$$\Delta E(^{+}CR^{-}) = {}^{2}IE_{v}(T) - RE_{v}(A^{+}) - EA_{v}(A') \quad (10)$$

Here, $^{2}IE_{v}(T)$ stands for the vertical double ionization energy of T (33.3 eV in the case of xenon) and $EA_{v}(A')$ is the vertical electron affinity of the neutral at the cation's geometry. Thus, the $^{+}CR^{-}$ process is rather energy demanding, and the onset of the anionic survivor signal is given by contributions due to $^{+}NR^{-}$, if the neutral species can be formed as a transient [27]; however, this is not always the case [28].

In the above considerations, a certain assumption is generally used in the energy balances of the NR processes. Thus, even though formed via vertical ET from an ion state, the neutrals are treated as if they reflect the properties of the ground state neutral. In Eq. (2), for example, the term $EA_{v}(A)$ is used rather than $EA_{v}(A')$ of a neutral species having the structure of the anion. This assumption is not just an approximation, but forms the essence of the NIDD approach in that during the microsecond flight time from the first to the second collision cell, the transient neutral is assumed to explore its entire rovibronic manifold where chemical reactivity and subsequent fragmentations are explicitly included in the NIDD technique. In other words, the transient neutral formed by vertical ET is assumed to relax to a system having electronic ground-state properties though with an elevated internal energy.

3.2. Energy-resolved NR and CR experiments on $NO^{-/+}$

Before entering the discussion, we shall briefly address the essentials of the potential energy surfaces $NO^{-/0/+}$. In the present context, only four states need to be considered: (i) the ground state anion NO^{-} ($^{3}\Sigma^{-}$) with a bond length of r = 1.27 Å [7], (ii) the neutral ground state radical $NO^{\bullet}$ ($^{2}\Pi$) with r = 1.15 Å [1,7], (iii) the ground state cation NO^{+} ($^{1}\Sigma^{+}$) with r = 1.06 Å [1], and (iv) the excited state cation NO^{+} ($^{3}\Sigma^{+}$) with r = 1.28 Å [1]. For the sake of simplicity, these are denoted in the following as $^{3}NO^{-}$, $^{2}NO^{\bullet}$, $^{1}NO^{+}$, and $^{3}NO^{+}$, respectively. As far as energetics are concerned, the relative (adiabatic) locations are $E_{rel}(^{2}NO^{\bullet})$ = 0.0 eV, $E_{rel}(^{3}NO^{-})$ = 0.026 eV, $E_{rel}(^{1}NO^{+})$ = 9.26 eV, and $E_{rel}(^{3}NO^{+})$ = 15.66 eV [1,7,8].

The survivor ion signal in the $^{-}NR^{-}$ experiment is characterized by a sharp feature (peak A in Fig. 1). As expected from Eq. (3), the onset of feature A (Table 2) is within experimental error of the IE of xenon which was used as the target gas. In addition, a second, much weaker feature B is observed which is of unknown origin; possible rationales involve collisional excitation of the target gas (e.g., $O_2 \rightarrow 2O$) or its double ionization, that is formation of $T^{2+} + e^{-}$ rather than T^{+} in Eq. (2). Similarly, the onset of the first feature (C) of the $^{+}NR^{+}$ survivor is consistent with IE(Xe) within experimental error, as expected from Eq. (6). A second, broader feature D of equal intensity is observed

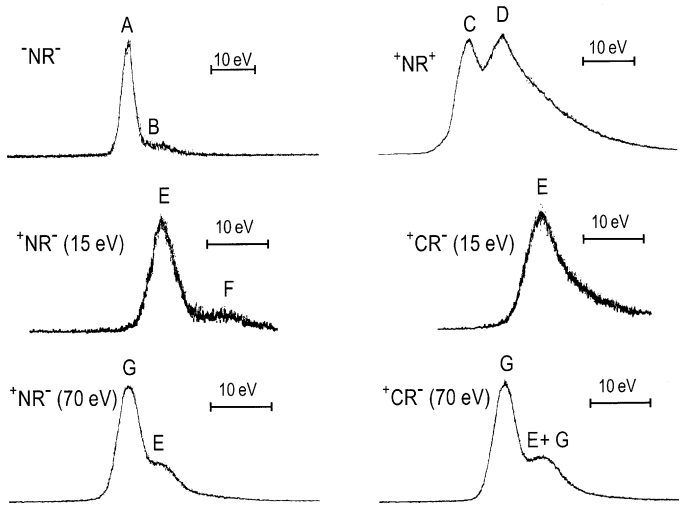

Fig. 1. Survivor ions in energy-resolved $^{-}NR^{-}$, $^{+}NR^{+}$, $^{+}NR^{-}$, and $^{+}CR^{-}$ spectra of $B(1)$-mass-selected $NO^{-/+}$ ions obtained by scanning $E(1)$. Note that the two latter experiments were performed by ionization of NO with electrons having two different energies (15 and 70 eV, see text). The various features observed are denoted as A–H. The energy scalings of the figures are indicated by the horizontal bar corresponding to a kinetic energy difference of 10 eV.

Table 2
Measured energy differences (ΔE in eV) of the various features of the survivor ion peaks[a] determined in energy-resolved NR and CR experiments[b] of $NO^{-/+}$ ions. In addition, the assigned transitions and their (adiabatic) energy balances are given

	Peak[a]	ΔE_{exp}[c]	Assignment	ΔE_{adia}[d]
$^{-}NR^{-}$	A	12.4 ± 0.5	$^{3}NO^{-} \rightarrow {}^{2}NO^{\bullet} \rightarrow {}^{3}NO^{-}$	12.1
	B	(19)[e]		
$^{+}NR^{+}$	C	12.0 ± 0.4	$^{1}NO^{+} \rightarrow {}^{2}NO^{\bullet} \rightarrow {}^{1}NO^{+}$	12.1
	D	19 ± 1	$^{1}NO^{+} \rightarrow {}^{2}NO^{\bullet} \rightarrow {}^{3}NO^{+}$	18.5
$^{+}NR^{-}$(15 eV)	E	15.5 ± 0.5	$^{1}NO^{+} \rightarrow {}^{2}NO^{\bullet} \rightarrow {}^{3}NO^{-}$	15.0
	F	(23)[e]		
$^{+}CR^{-}$(15 eV)	E	15.7 ± 0.5	$^{1}NO^{+} \rightarrow {}^{2}NO^{\bullet} \rightarrow {}^{3}NO^{-}$	15.0
			$^{1}NO^{+} + Xe \rightarrow {}^{3}NO^{-} + Xe^{2+}$	24.1
$^{+}NR^{-}$ (70 eV)	G	9.4 ± 0.5	$^{3}NO^{+} \rightarrow {}^{2}NO^{\bullet} \rightarrow {}^{3}NO^{-}$	8.6
$^{+}CR^{-}$ (70 eV)	G	9.8 ± 0.5	$^{3}NO^{+} \rightarrow {}^{2}NO^{\bullet} \rightarrow {}^{3}NO^{-}$	8.6
	H		$^{3}NO^{+} + Xe \rightarrow {}^{3}NO^{-} + Xe^{2+}$	17.7
$^{-}NR^{+}$	I	9.2 ± 0.5	$^{3}NO^{-} \rightarrow {}^{1}NO^{+}$	9.2
	J	16 ± 1	$^{3}NO^{-} \rightarrow {}^{3}NO^{+}$	15.6
$^{-}CR^{+}$	I	9.5 ± 0.5	$^{3}NO^{-} \rightarrow {}^{1}NO^{+}$	9.2
	J	16 ± 1	$^{3}NO^{-} \rightarrow {}^{3}NO^{+}$	15.6

[a] For a designation, see Fig. 1.
[b] The charges of the projectile and product ions are indicated as superscripts.
[c] Errors of ±0.5 eV for ΔE values determined from the onsets of the survivor signals and ±1 eV for secondary features.
[d] For the sake of simplicity, the corresponding adiabatic transitions are considered here; see text.
[e] Assignment of the onset is uncertain due to strongly overlapping features and/or peak broadening.

ca. 7 eV higher in energy and is assigned to the formation of $^3NO^+$ upon collisional reionization of the neutral molecule. Interestingly, the overall shape of the $^+NR^+$ survivor signal does not depend on the projectile ions in that EI of NO with electrons having either 15 or 70 eV as well as dissociative EI of N_2O (at 70 eV) give similar patterns.

In contrast, a remarkable dependence from the ionization conditions is observed in the $^+NR^-$ and $^+CR^-$ experiments. At an ionization energy of 15 eV, only the $^1NO^+$ cation can be formed from neutral nitrogen monoxide. The corresponding $^+NR^-$ (15 eV) signal shows two features (E and F) of which the first is assigned to the ground-to-ground state transition $^1NO^+ \rightarrow {}^2NO^\bullet \rightarrow {}^3NO^-$ (Table 2); the second, much weaker and broader component is similar to feature B in $^-NR^-$ and also is not assigned to a particular process. The $^+CR^-$ (15 eV) signal is dominated by NR processes. The broader tail of the $^+CR^-$ peak compared to $^+NR^-$ can be assumed to reflect some contribution of the direct charge reversal $^1NO^+ + Xe \rightarrow {}^3NO^- + Xe^{2+}$ which takes 9 eV more energy than the stepwise $^+NR^-$ sequence. At an ionization energy of 70 eV, however, the $^+NR^-$ and $^+CR^-$ signals show an additional component G which appears at a considerably lower DE value than that of the adiabatic ground-to-ground state transition. Accordingly, feature G is attributed to the excited $^3NO^+$ state for which the neutralization step is more favorable. This interpretation is in agreement with the onsets of the $^+NR^-$ and $^+CR^-$ signals at 70 eV ionization energy, though the measured values are slightly larger than expected for the adiabatic transitions (Table 2). Whereas the first features in the 70 eV $^+NR^-$ and $^+CR^-$ spectra are almost superimposable, the second peak is significantly broadened in $^+CR^-$, which is assigned to E along with some contribution of the direct charge reversal $^3NO^+ + Xe \rightarrow {}^3NO^- + Xe^{2+}$(H). We note in passing that generation of NO^+ by dissociative EI of N_2O at 70 eV gives an intermediate situation (not shown) in which feature E prevails while G is observed already. Accordingly, the relative yield of $^3NO^+$ is lower for dissociative ionization of N_2O with 70 eV electrons than for EI (70 eV) of neutral NO itself, which is a reasonable scheme.

An obvious question is why the presence of $^3NO^+$ in the precursor beam hardly affects the $^+NR^+$ signal while it exhibits a dramatic influence in $^+NR^-$ and $^+CR^-$ experiments. The answer to this question has two facets. At first, energy-resolved $^+NR^+$ (as well as $^-NR^-$) experiments are a priori insensitive towards the nature of the precursor ions. Thus, neutralization of excited $^3NO^+$ is of course, much easier than that of the ground state cation, but would lead to a highly excited neutral which, in turn, is much easier to ionize. Provided that the intermediate neutral cannot loose internal energy by radiative processes or chemical transformations (both unlikely/impossible for NO), these contributions therefore cancel each other in the overall energy balances of NR experiment with no changes in the overall charge states. The second aspect is more specific to the $NO^{-/0/+}$ system. Thus, $^3NO^+$ and $^3NO^-$ show an almost perfect match of the bond distances (see above) such that their interconversion (with or without neutral intermediate) is likely to be efficient. In comparison, the N–O distance in the ground state cation $^1NO^+$ is much shorter and hence expected to be associated with much less favorable Franck–Condon factors for the conversion to the anionic species.

While the differences between the $^+NR^-$ and $^+CR^-$ experiments are gradual, a pronounced difference is found for the $^-NR^+$ and $^-CR^+$ survivors (Fig. 2). The $^-NR^+$ signal is characterized by two, relatively sharp features (I and J) of equal heights, whereas both components are much broader upon $^-CR^+$, and feature I is significantly less pronounced compared to J. Based upon the measured onsets, I and J are assigned to the transitions $^3NO^- \rightarrow {}^1NO^+$ and $^3NO^- \rightarrow {}^3NO^+$, respectively (Table 2). The pronounced differences are also reflected in the corresponding energy-resolved $^-NIDD^+$ spectrum shown at the bottom of Fig. 2, showing a large positive component for I and a negative one for J. The intermediate oscillation is associated with the different widths of the $^-NR^+$ and $^-CR^+$ components.

In order to explain this difference, consider the redox processes in terms of schematic potential energy

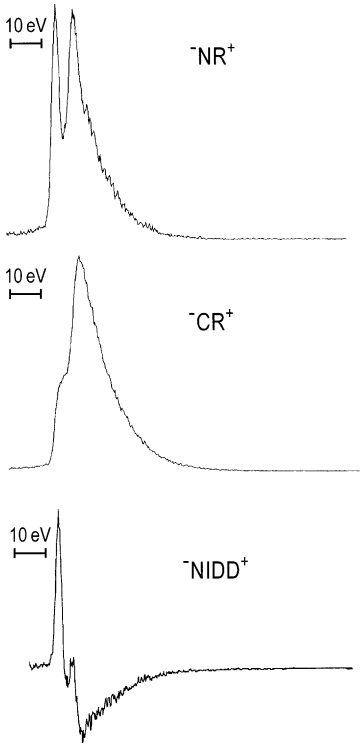

Fig. 2. $^{-}NR^{+}$, $^{-}CR^{+}$, and resulting $^{-}NIDD^{+}$ spectra of *B*(1)-mass-selected NO^{-} generated from N_2O obtained by scanning *E*(1); for details of the NIDD procedure, see [10–13]. The energy scaling is indicated by the horizontal bar corresponding to a kinetic energy difference of 10 eV.

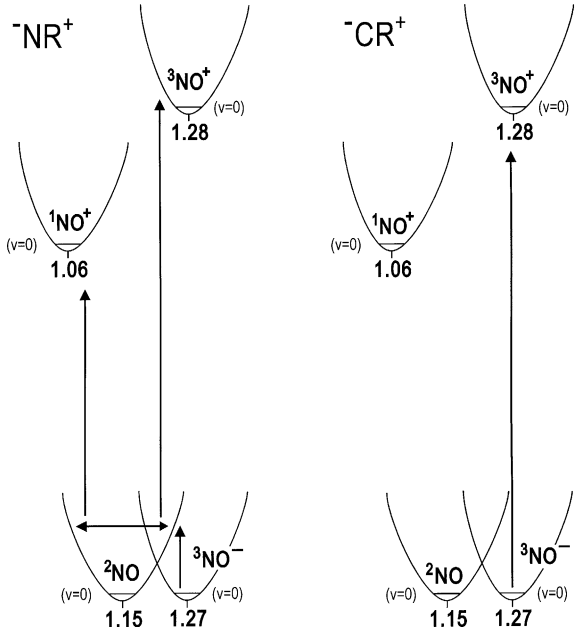

Fig. 3. Schematic potential energy curves of $NO^{-/0/+}$ [1,7] showing the electron-transfer processes involved in the $^{+}NR^{-}$ and $^{-}CR^{+}$ experiments, respectively.

curves (Fig. 3). The first step in $^{-}NR^{+}$ corresponds to collisional electron detachment from $^{3}NO^{-}$. According to potential energy curves calculated by Griffith and coworkers [7], vertical detachment is most likely to yield $^{2}NO^{\bullet}$ ($v = 2 \pm 1$). During the passage from the first to the second collision cell, this vibrational level is explored such that upon reionization both $^{1}NO^{+}$ and $^{3}NO^{+}$ can be formed. In contrast, formation of the ground state cation by direct $^{-}CR^{+}$ without a neutral intermediate is much less likely, whereas $^{-}CR^{+}$ to $^{3}NO^{+}$ can proceed even more efficiently. This line of reasoning also accounts for the different widths of the $^{-}NR^{+}$ and $^{-}CR^{+}$ components in that ionization of neutral $^{2}NO^{\bullet}$ with $v = 2 \pm 1$ is likely to yield specific vibrational levels of the cations formed, whereas direct $^{-}CR^{+}$ to $^{1}NO^{+}$ leads to higher vibrational levels in feature I. Finally, the broadening of component J upon $^{-}CR^{+}$ can tentatively be attributed to enhanced collisional excitation of $^{3}NO^{+}$ due to the lower vibrational spacing in the triplet state as well as the formation of other excited states of NO [1].

4. Conclusions

While the present experiments demonstrate that $NO^{-/+}$ ions can successfully be subjected to all conceivable kinds of NR and CR experiments, these electron transfer processes do not provide any new information about the chemistry and physics of nitrogen monoxide. In turn, the knowledge of the properties of nitrogen monoxide can be used to test the performance of energy-resolved experiments. Hence, ET-MS is suitable to examine the energy balances of redox processes with an accuracy within the electron-volt regime. More precise determinations require sufficient precursor and survivor ion currents as well as complementary, reliable quantum mechanical data in order to assess the effects of vertical and adiabatic

transitions. Further, additional work on the calibration schemes used in energy-resolved experiments and the assignment of some high-energy features is required. Notwithstanding these apparent limitations, energy-resolved ET-MS experiments can be used to determine the redox properties of gaseous species which are difficult to probe by other spectroscopic means, e.g., distonic ions [23], biradicals [28,34], and coordinatively unsaturated transition-metal compounds [22,25,35].

Finally, the comparison of the energy-resolved $^{-}NR^{+}$ and $^{-}CR^{+}$ spectra of NO^{-} has two important conclusions as far as ET-MS is concerned in general. Firstly, the difference between the $^{-}NR^{+}$ and $^{-}CR^{+}$ signals provides direct evidence for the structural relaxation of the transient neutrals in NR experiments, thereby confirming a key assumption of the NIDD technique [13]. Secondly, even in cases where the overall NR and CR spectra are identical, the survivor ions need not necessarily be the same.

Acknowledgements

This work was supported by the Deutsche Forschungsgemeinschaft, the Fonds der Chemischen Industrie, and the Gesellschaft von Freunden der Technischen Universität Berlin. Further, we thank Dr. Kelly S. Griffith for providing preliminary data on the electron affinity of NO and Dr. Stephen. J. Blanksby as well as Dr. Thomas Weiske for helpful assistance in the experiments and data treatment.

References

[1] D.L. Albritton, A.L. Schmeltekopf, R.N. Zare, J. Chem. Phys. 71 (1979) 3271.
[2] E.E. Ferguson, J. Phys. Chem. 90 (1986) 731.
[3] S. Fenistein, M. Heininger, R. Marx, G. Mauclaire, Y.M. Yang, Chem. Phys. Lett. 172 (1990) 89.
[4] T. Wyttenbach, C.G. Beggs, M.T. Bowers, Chem. Phys. Lett. 177 (1991) 239.
[5] W. Lindinger, Int. J. Mass Spectrom. Ion Process. 80 (1987) 115.
[6] A. Hansel, N. Oberhofer, W. Lindinger, V.A. Zenevich, G.D. Billing, Int. J. Mass Spectrom. Ion Process. 185–187 (1999) 559.
[7] M.C. McCarthy, J.W.R. Allington, K.S. Griffith, Chem. Phys. Lett. 289 (1998) 156, and references cited therein.
[8] See: http://webbook.nist.gov.
[9] R.G. Cooks, J.H. Beynon, T. Ast, J. Am. Chem. Soc. 94 (1972) 1004.
[10] C.A. Schalley, Gas-Phase Ion Chemistry of Peroxides, Dissertation, Technische Universität Berlin D83, Shaker, Herzogenrath/Germany, 1997.
[11] G. Hornung, C.A. Schalley, M. Dieterle, D. Schröder, H. Schwarz, Chem. Eur. J. 3 (1997) 1866.
[12] C.A. Schalley, G. Hornung, D. Schröder, H. Schwarz, Chem. Soc. Rev. 27 (1998) 91.
[13] C.A. Schalley, G. Hornung, D. Schröder, H. Schwarz, Int. J. Mass Spectrom. 172/173 (1998) 181.
[14] N. Goldberg, H. Schwarz, Acc. Chem. Res. 27 (1994) 347.
[15] M.M. Bursey, Mass Spectrom. Rev. 9 (1990) 555.
[16] A.S. Dannell, G.L. Glish, Int. J. Mass Spectrom. 212 (2001) 219.
[17] C.A. Schalley, D. Schröder, H. Schwarz, Int. J. Mass Spectrom. Ion Process. 153 (1996) 173.
[18] D. Schröder, J. Loos, M. Semialjac, T. Weiske, H. Schwarz, G. Höhne, R. Thissen, O. Dutuit, Int. J. Mass Spectrom. Ion Process. 214 (2002) 155.
[19] D. Schröder, H. Schwarz, J. Phys. Chem. A 103 (1999) 7385.
[20] S. McCullough-Catalano, C.B. Lebrilla, J. Am. Chem. Soc. 115 (1993) 1441, and references cited therein.
[21] D. Schröder, S. Bärsch, H. Schwarz, J. Phys. Chem. A 104 (2000) 5101.
[22] J.N. Harvey, C. Heinemann, A. Fiedler, D. Schröder, H. Schwarz, Chem. Eur. J. 2 (1996) 1230.
[23] D. Schröder, N. Goldberg, W. Zummack, H. Schwarz, J.C. Poutsma, R.R. Squires, Int. J. Mass Spectrom. Ion Process. 165/166 (1997) 71.
[24] D. Schröder, J.N. Harvey, M. Aschi, H. Schwarz, J. Chem. Phys. 108 (1998) 8446.
[25] D. Schröder, S. Bärsch, H. Schwarz, Int. J. Mass Spectrom. 192 (1999) 125.
[26] D. Schröder, C.A. Schalley, N. Goldberg, J. Hrušák, H. Schwarz, Chem. Eur. J. 2 (1996) 1235.
[27] J.N. Harvey, D. Schröder, H. Schwarz, Bull. Soc. Chim. Belge 106 (1997) 447.
[28] D. Schröder, C. Heinemann, H. Schwarz, J.N. Harvey, S. Dua, S.J. Blanskby, J.H. Bowie, Chem. Eur. J. 4 (1998) 2550.
[29] N. Jeffreys, I.W. Griffiths, D.E. Parry, F.M. Harris, Chem. Phys. Lett. 266 (1997) 537, and references cited therein.
[30] D. Schröder, K. Schroeter, W. Zummack, H. Schwarz, J. Am. Soc. Mass Spectrom. 10 (1999) 878.
[31] D. Schröder, K. Schroeter, H. Schwarz, J. Phys. Chem. A 103 (1999) 4174.
[32] R. Srinivas, S. Vivekananda, S.J. Blanksby, D. Schröder, H. Schwarz, L.M. Fell, J.K. Terlouw, Int. J. Mass Spectrom. 197 (2000) 105.
[33] J.H. Bowie, Int. J. Mass Spectrom. 212 (2001) 249.
[34] S.J. Blanksby, D. Schröder, S. Dua, J.H. Bowie, H. Schwarz, J. Am. Chem. Soc. 122 (2000) 7105.
[35] P. Jackson, J.N. Harvey, D. Schröder, H. Schwarz, Int. J. Mass Spectrom. 204 (2001) 233.